Electronics and Communications in Japan, Part 1, Vol. 88, No. 8, 2005
Translated from Denshi Joho Tsushin Gakkai Ronbunshi, Vol. J87-B, No. 9, September 2004, pp. 1336–1345

Radiation and Ohmic Resistances in Very Small Meander Line Antennas of Less than 0.1 Wavelength

Masato Takiguchi and Yoshihide Yamada

Department of Electrical and Electronic Engineering, National Defense Academy, Yokosuka, 239-8686 Japan

SUMMARY

Demands for extremely small antennas to be used in radiofrequency identification tags for ubiquitous communication have increased. Examples of very small antennas utilizing meander line structures are seen. To date, important studies have been carried out on basic design and on improvement of the radiation efficiency by a folded configuration. Most of the structures studied have dimensions of more than 0.1 wavelength. For the demands of ultracompact antennas, this paper deals with meander line antennas whose dimensions are less than 0.1 wavelength. First, the parameters for resonant configurations are derived for antennas with dimensions of 0.1 to 0.025 wavelength. Next, the radiation resistance and the ohmic resistance are studied in the folded structures. First, through a transmission line model analysis, it is shown that the step-up ratios of radiation and ohmic resistances in the case of folded structures are different. In addition, these resistances that are basic values of electrical performances are derived through electromagnetic simulations. Further, in order to confirm the validity of the numerical results and the realizable performance, antennas with dimensions of 0.1 and 0.05 wavelength were fabricated. Electrical characteristics are compared, and good agreements are found. © 2005 Wiley Periodicals, Inc. Electron Comm Jpn Pt 1, 88(8): 1–11, 2005; Published online in Wiley InterScience (www.interscience.wiley.com). DOI 10.1002/ecja.20204

Key words: meander line antenna; folded structure; step-up ratio; radiation resistance; ohmic resistance.

1. Introduction

Recently, demands for extremely small antennas for use in IC tags for ubiquitous communications have increased. Well-known very small antennas are small loop antennas for pagers [1]. The antenna dimension is about 0.05 wavelength with an extremely low gain of –18 dBd [2]. Also, since the antenna input impedance has a large inductance component, it is necessary to add a capacitive component for use. Other excellent antennas with improved gain and self-resonance characteristics are the normal mode helical antenna [3] and the meander line antenna [4]. The normal mode helical antenna has a coil structure and requires a three-dimensional configuration. Since the meander line antenna has a two-dimensional configuration consisting of conductors meandering on a planar surface, it has good fitness to a sheet circuit. When application to IC tags is considered, planar structure is a significant condition, so that the meander line antenna is promising.

An example of a meander line antenna applied to IC tags has been reported, but its electrical characteristics were not shown [5]. Antenna design and electrical characteristics were shown in the following studies. (1) Endo and colleagues expressed the resonant condition of a small meander line antenna with a size of more than 0.1 wavelength in forms of a transcendental equation with the number of meander stages and the antenna length and width as variables. They studied various resonant structures and showed that the radiation efficiency decreases quickly if the antenna length becomes less than 0.1 wavelength [6]. (2) Noguchi and colleagues fabricated meander line antennas with a size of more than 0.15 wavelength and obtained a radiation resistance of more than 5 Ω [7]. It has also been shown that

the radiation resistance can be increased by a factor of 4 if a folded structure is used [8]. In order to meet demands for further size reduction, it is necessary to determine the structural parameters of an antenna with a size of less than 0.1 wavelength and to study the realizability of the electrical characteristics.

In this paper, an antenna with a size of less than 0.1 wavelength is designed and the realized characteristics are found by measurement. In Section 2, the self-resonance structure and input resistance are derived by electromagnetic simulation for antennas with a size of 0.025 to 0.1 wavelength. In Section 3, improvement of the electrical characteristics by the use of a folded configuration is studied with respect to the physical meaning and achieved values. In Sections 4 and 5, measured data for fabricated antennas with sizes of 0.1 and 0.05 wavelength are presented.

2. Basic Meander Line Antenna

2.1. Dimensional parameters and input resistance at resonance

The basic configuration of the meander line antenna is shown in Fig. 1. The antenna length is L and the width is W. The number of stages (N) of the meander line is the total of the bent sections and is 10 in this case. The other antenna parameters are d for the conductor width and s for the conductor spacing. L_f is the separation of the left and right meander sections and is greater than 2 mm to allow for coaxial cable feed. Δ is the segmentation length used in the method of moments in order to calculate the current distributions; it has a value of one to several tenths of a wavelength. In the meander sections, the conductors are started bending at both ends of the antenna and bended conductors are arranged so as to have uniform spacing s within the L–L_f regions. The frequency used in this study is 700 MHz, close to that of portable phones.

In designing an antenna to have high efficiency, the conductor width (d) plays an important role. The maximum conductor width available is determined using parameters of the antenna length (L) and N. At 700 MHz, the maximum width (d_{max}) of the conductors for $s = 0.1$ mm (2.3×10^{-4} λ) are shown in Fig. 2. It is seen that the conductor widths are reduced when the antenna lengths are made shorter. When the antenna length is reduced to 0.025 wavelength with N = 38, d_{max} because 0.105 mm (2.3×10^{-4} λ). On the other hand, when N = 38 at 0.05 wavelength, d_{max} can be increased up to 0.374 mm (8.7×10^{-4} λ).

Figure 3 shows the self-resonance conditions of the antenna lengths and antenna widths. The calculations were made with an electromagnetic simulator (IE3D) based on the method of moments. The reliability of the numerical values is judged by the convergence of the numerical results for the input impedance of the antenna. The convergence was evaluated for an antenna with L = 0.05 λ. As the numerical segmentation length Δ is reduced, the numerical accuracy is significantly increased. According to the numerical results of the input impedance in the range of $10 \leq \lambda/\Delta \leq 80$, convergence is obtained at $\lambda/\Delta = 20$. Since stable convergence occurs when λ/Δ is more than 40, subsequent calculations were carried out with $\lambda/\Delta = 40$. At $\lambda/\Delta = 40$, Δ is small enough that at least two Δ can fit within W, even if W has its smallest size. Figure 3 shows the results for conductor widths (d) of 0.1 mm (2.3×10^{-4} λ) and 0.3 mm (7.0×10^{-4} λ). When d = 0.3 mm and N = 38, there is a lack of data for L/λ = 0.025. This is because the structure is possible only for $L/\lambda > 0.05$ if d = 0.3 mm, as is evident from Fig. 2. When the conductor width (d) is tripled, the antenna width (W) increases by about 30%. For a reduction of the antenna length, the antenna width increases almost linearly. It is also found that the antenna width can be designed smaller for a larger number of stages if the antenna

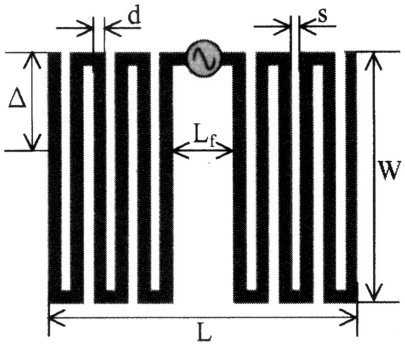

Fig. 1. Configurations of meander line antenna.

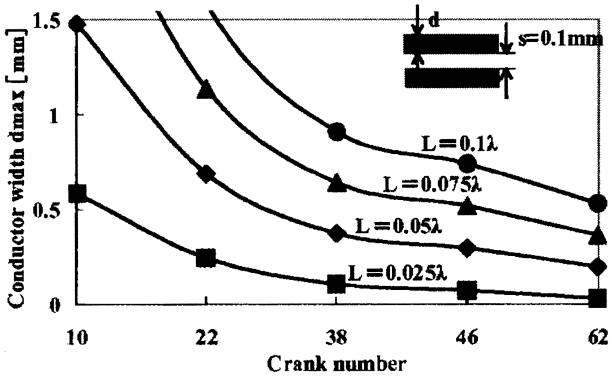

Fig. 2. Limits of conductor width.

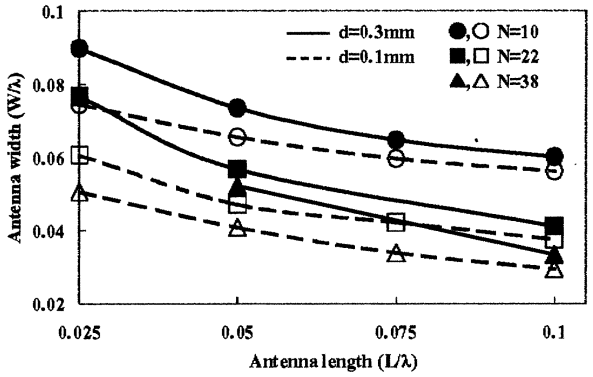

Fig. 3. Antenna length and width of resonance point.

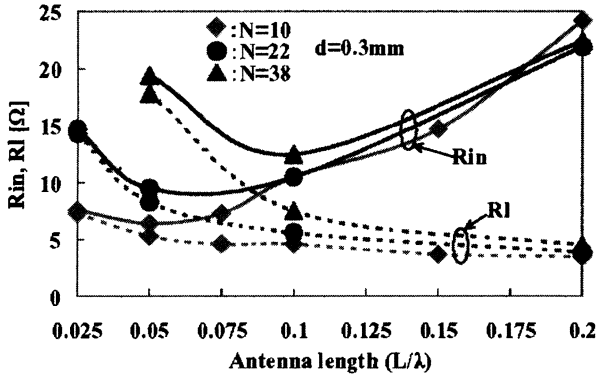

Fig. 5. Input resistances and ohmic resistances of conventional configuration.

length remains constant. From the relationship between the antenna length (L) and the antenna width (W), it is found that $W > L$ if the antenna length is smaller than 0.05 wavelength. In order to realize a small antenna with $L = W$, the values of N must be increased further.

Figure 4 shows the total length (L_a) of the antenna conductor at self-resonance. As the conductor width (d) is increased, the conductor length (L) needed is increased. If L is to be reduced, L_a must be made longer. The incremental rate is higher for larger N. Also, as N is increased, L_a is increased. Here, it should be noted that L_a lies in the region of 1 to 2 wavelengths.

Figure 5 shows the input resistance (R_{in}) and the ohmic resistance (R_l) when the conductor width (d) is 0.3 mm (7.0×10^{-4} λ). As shown in Eq. (1), the ohmic resistance is known by subtracting the input resistance for infinite conductivity ($\sigma = \infty$) from the input resistance of the conductivity of copper (σ_c). In this case, the radiation resistance (R_r) is equal to the input resistance for infinite conductivity ($\sigma = \infty$):

$$R_l = R_{in}(\sigma_c) - R_{in}(\sigma = \infty) \tag{1}$$

In Fig. 5, resistance changes of R_{in} and R_l due to N are small when the length is more than 0.1 wavelength. Below 0.1 wavelength, R_l increases quickly as L becomes smaller when N is large. It is also found that the radiation resistance given by $R_{in} - R_l$ decreases quickly in accordance with the reduction of antenna length. As shown in Eq. (2), the ohmic resistance varies with the total length of the conductor (L_a), the conductor width (d), and the frequency (f):

$$R_l = \frac{L_a}{2(d+t)\delta} \cdot \frac{1}{\sigma}, \quad \delta = \sqrt{\frac{1}{f\pi\mu\sigma}} \tag{2}$$

Here, t is the conductor thickness and δ is the skin depth of the conductor. When $\sigma_c = 5.8 \times 10^7$ S/m of copper is used for the conductivity, δ = 2.5 μm at 700 MHz. The value of t is chosen as 35 μm in consideration of the actual copper film thickness, which is sufficiently larger than δ. The peculiar dependences of R_l on variables are such that R_l changes in inverse proportion to d and is proportional to L_a and $\sqrt{f}$. The reason that R_l increases remarkably below 0.1 wavelength is the increase of L_a at large N values. For $L/\lambda = 0.05$, R_l of $N = 38$ is more than twice that of other numbers of stages.

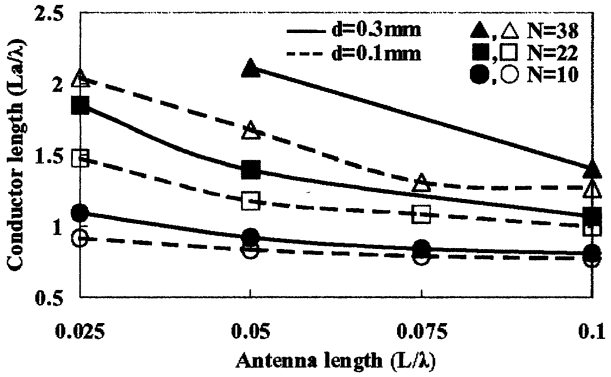

Fig. 4. Antenna length and conductor length.

2.2. Comparison with conventional design equation

With regard to the self-resonance structure of the antenna, the following convenient design equation is given in Ref. 6:

$$wN_0 \log\frac{L}{N_0 b} + \frac{L}{2}\left(\log\frac{4L}{b} - 1\right) = \frac{\lambda}{4}\left(\log\frac{2\lambda}{b} - 1\right) \quad (3)$$

where L is the antenna length, w is the antenna width, N_0 is the number of stages, and b is the diameter of the conductor rod. The left-hand side of the above equations expresses the inductance of the meander line antenna. This is given by the sum of the inductance of $2N_0$ crank sections and the self-inductance of an infinitesimal dipole antenna with a length of L. The right-hand side is equal to the self-inductance of a half-wave dipole with the same frequency. If the resonant frequency is identical, it is assumed that the inductance of the meander line antenna is equal to that of the half-wave dipole antenna.

Figure 6 shows a comparison of the results obtained from design equation (3) and the present simulation. Here, $N = 2N_0$ and the value of b is set equal to the width (d) of the meander line and is 0.3 mm (7.0×10^{-4} λ). When $b > d$, numerical values of Eq. (3) for W, indicated by the dotted line, shift in the upward (increasing) direction. On the other hand, results of Eq. (3) shift downward for $b < d$. In the case of $b = d$, the simulation value and the results of Eq. (3) coincide at $N = 22$ and $N = 38$. The difference between the dotted line and the solid line is largest when $N = 10$ at $L/\lambda = 0.05$. The difference is at most 20%. The diameter (b) of the conductor rod is usually considered equivalent to the conductor width (d) when $2b \approx d$. In the present comparison, the feed spacing is chosen large for the antenna structure in simulation, as shown in Fig. 1. The structure is slightly different from the model for Eq. (3), in which the meander sections are uniformly placed within L. Therefore, the numerical results happen to be coincident when b is chosen as d instead of $d/2$. Although the present comparison is not rigorous, the effectiveness of Eq. (3) can be recognized.

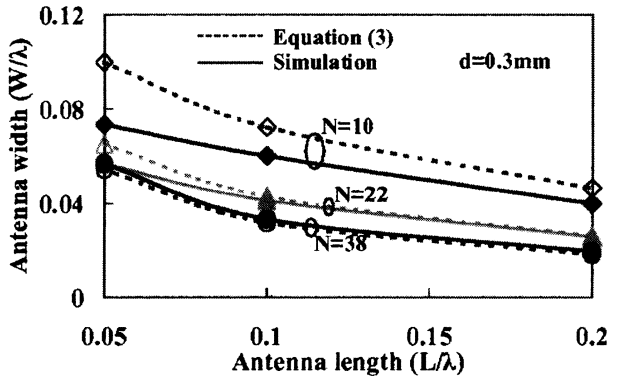

Fig. 6. Resonance structures.

3. Input Resistance of Folded Structure

3.1. Folded structure

It is stated in Ref. 9 that the radiation resistance can be made four times if the meander line antenna is modified to a folded structure. The folded structures in Figs. 7(a) and (b) are typical. The overlapped form is the one studied in Ref. 8. Since the electrical characteristics are almost identical in these two structures [9], the parallel form, representing the basic configuration, is treated here.

3.2. Step-up ratio of radiation resistance and ohmic resistance

3.2.1. Derivation by transmission line model

The electrical characteristics of the folded dipole antenna can be considered by replacing it with two transmission line models, asymmetrical and symmetrical, and can be represented by Figs. 8(a) and 8(b) [10]. Let the input resistances of these modes be Z_t and Z_a. Also, let the input resistance of the folded dipole antenna be Z_f. Then, $Z_f = 4Z_tZ_a/(2Z_a + Z_t)$, as shown in Eq. (4). Let us consider a half-wave folded dipole antenna. In the case of the asymmetric mode, the resistance (Z_t) whose end is short terminated becomes infinite. Hence, as shown by Eq. (5), $Z_f = 4Z_a$. In this way, only the input resistance (Z_a) of the symmetric mode must be considered when only the input resistance of the folded dipole antenna at resonance is considered.

In the case of the symmetric mode, since the directions of the current flows in the twin parallel wires are equal, the twin parallel wires can be replaced with a thick conductor as shown in Fig. 8(c). The input resistance (Z_a) of the symmetric mode can be expressed by the two terms of the

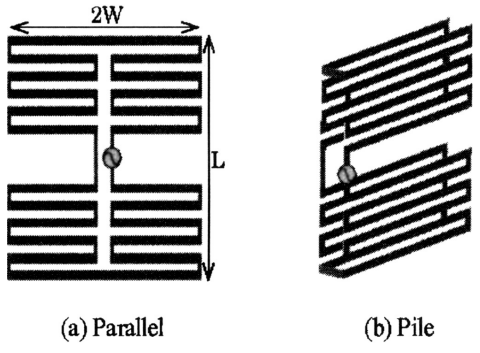

Fig. 7. Folded structures.

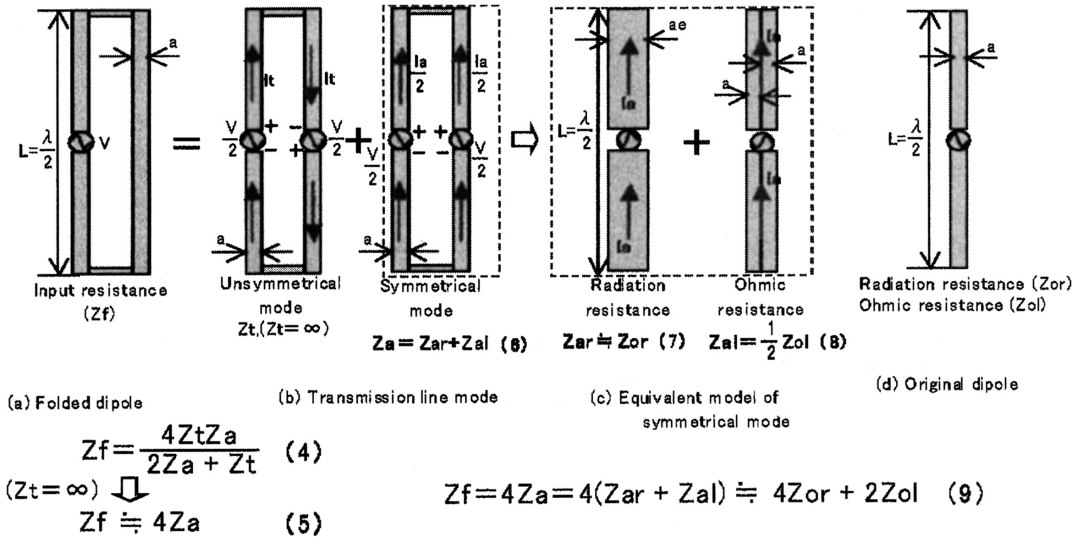

Fig. 8. Study of step-up ratio by transmission line mode.

radiating resistance (Z_{ar}) and the ohmic resistance (Z_{al}). These values have an important relationship with the resistances of the original dipole antenna [Fig. 8(d)]. Let the radiation resistance and the ohmic resistance of the original dipole antenna be Z_{or} and Z_{ol}. The relationship between the symmetric mode and the original dipole antenna for the radiation resistance is $Z_{ar} \approx Z_{or}$, as shown in Eq. (7), because the antenna lengths are equal even though the conductor widths are slightly different. Also, the relationship between the symmetric mode and the original dipole antenna in the conducting resistance is $Z_{al} = Z_{ol}/2$, as shown in Eq. (8), because the model for the ohmic resistance of the symmetric mode is twice the conductor width of the dipole antenna. In Eq. (9), when the values from Eqs. (7) and (8) are substituted, we obtain $Z_f = 4Z_{ar} + 2Z_{ol}$. Hence, the step-up ratio of the radiation resistance of the folded dipole antenna is a factor of 4, while that of the ohmic resistance is a factor of 2.

3.2.2. Validity of the transmission line model

In this section, we study by simulation whether the transmission line model is applicable to the folded meander line antenna. In Fig. 9(a), a model with the asymmetric mode feed of Fig. 8(b) for the folded meander line antenna in Fig. 7(a) is presented. The direction of the current is indicated by arrows. The current distribution is obtained by compressing and folding the current in Fig. 8(b) in the L direction. The current flows in the W direction are opposite in adjacent conductors. The input impedance characteristics are shown in Fig. 9(b). In the case of the meander line antenna, it is also confirmed that the resistance values for 600 to 800 MHz tend to infinity and the input impedance Z_t for the asymmetric mode is $Z_t = \infty$. As a result, it is expected that the asymmetric mode will not be excited and that only the symmetric mode will exist also in the meander line antenna.

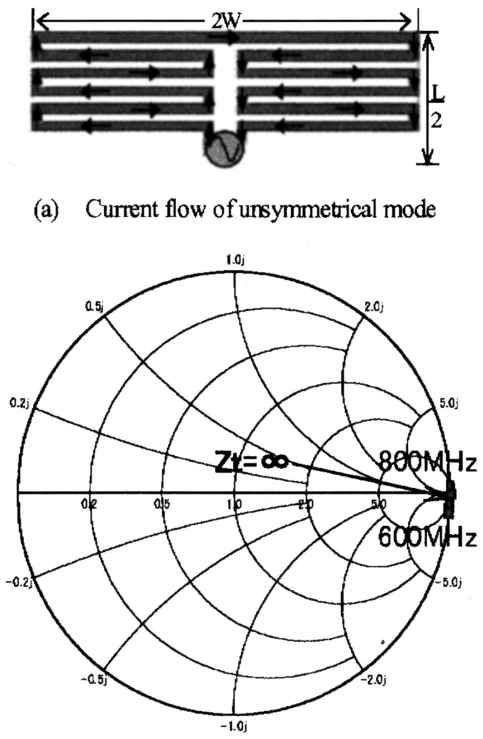

Fig. 9. Current flow and input impedance of unsymmetrical mode.

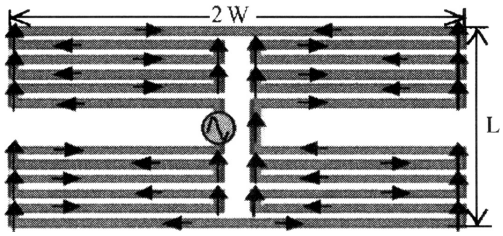

Fig. 10. Current flow of symmetrical mode.

Figure 10 shows the current distributions in the folded meander line antenna with arrows. The current distributions of the symmetric mode in Fig. 8(b) are folded in the *L* direction and compressed. The orientations of the currents are opposite in adjacent conductors. Along *L*, all currents are in the same direction. It is seen that the currents in the *L* direction are the radiation source.

3.3. Antenna input resistance value

3.3.1. Computed value of the step-up ratio

The values of the radiation resistance (R_r) and the ohmic resistance (R_l) contained in the input resistance (R_{in}) of the folded configuration are shown in Fig. 11. The step-up ratio is derived by comparison with the values in Fig. 5 of N = 10. Here, the ohmic resistance is calculated from Eq. (1). It is found that the input resistance [$R_{in}(f)$] of the folded structure is higher than that of the conventional configuration [$R_{in}(o)$]. The value of the radiation resistance is the difference between the solid line and the broken line. When radiation resistances of the conventional configuration [$R_r(o)$] and the folded configuration [$R_r(f)$] are compared, a step-up ratio of about 4 is obtained for all antenna lengths. Next, the step-up ratio of the ohmic resistances is

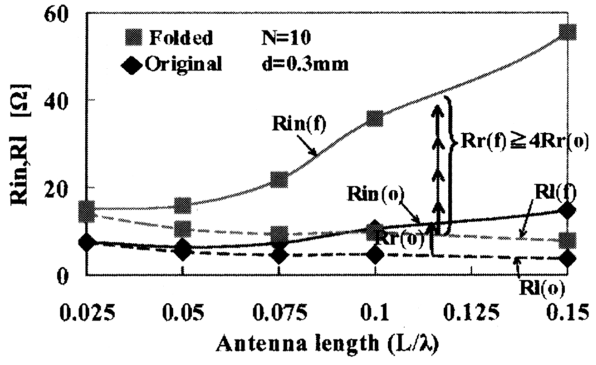

Fig. 11. Step-up ratio of folded structures.

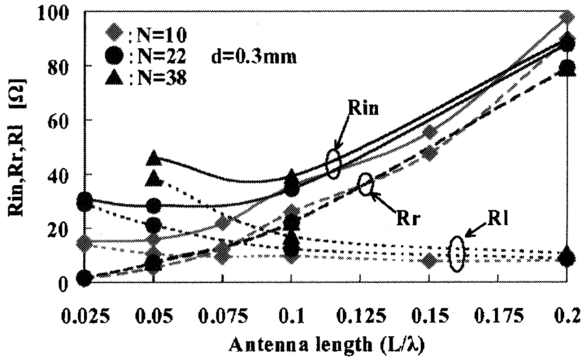

Fig. 12. Resistances of folded structure.

found to be about 2 when the conventional configuration [$R_l(o)$] and the folded configuration [$R_l(f)$] are compared.

3.2.2. Numerical value of the antenna input resistance

Figure 12 shows the variation of the resistance value as N is varied. For N of 10, 22, and 38, the antenna length is varied from 0.025 λ to 0.2 λ. It is found that the radiation resistance (R_r) does not change with N at any value of L. Hence, N does not influence the increase in R_r. As the antenna length is reduced, R_r changes significantly. The ohmic resistance (R_l) increases with N, since the total length (L_a) of the conductor varies by N as shown in Fig. 4. An important characteristic is that there exists a point at which R_l is larger than R_r. As N is increased, the crossing point occurs at longer antenna lengths. It is concluded that the radiation efficiency is degraded as N is increased, even though the antenna size can be reduced.

4. Trial Fabrication of 0.1 λ Antenna

4.1. Measured results of input resistance

Figure 13 shows the fabricated antenna used for experiments. The dimensions are: N = 10, L = 43 mm (0.1λ), W = 35 mm (0.08 λ), L_f = 10 mm (0.02 λ), d = 1.7 mm (4.0 × 10^{-3} λ), and s = 1.4 mm (3.3 × 10^{-3} λ). Both the conventional structure and the folded structure were built. The conductor was a copper film with a thickness of 0.1 mm (2.3 × 10^{-4} λ). In the experiment, many values were intended to be compared with the simulation results in various aspects. Therefore, in consideration of the temperature variations of the ohmic resistance, measurements was performed at room temperature and at a cooled temperature. For cooling, liquid nitrogen was poured into the bottom of

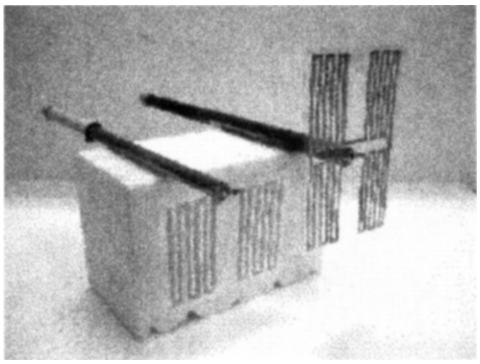

Fig. 13. Manufactured 0.1 λ antennas.

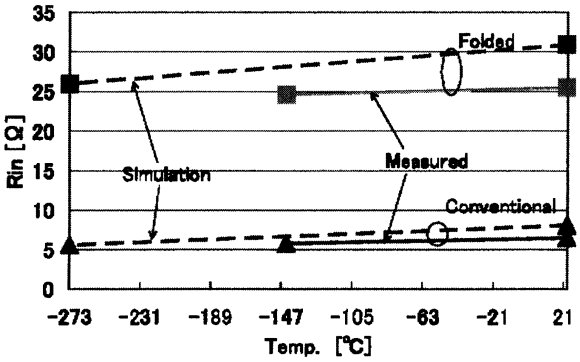

Fig. 15. Temperature versus input resistances (0.1 λ).

a Styrofoam box and the antenna to be measured was suspended in space. The box was closed by a lid and the antenna was cooled with nitrogen vapor [11]. The temperature obtained was –144 °C. Figure 14 shows the measured input impedance values. The input resistance at resonance was 1 Ω lower when cooled. In order to increase the reliability of the measured values, a structure employing the electrical image was measured in addition to the structure fed by a coaxial cable. The measured values of the conventional and folded configurations were almost equal to the values of Fig. 14 at room temperature and the cooled temperature conditions [11]. Hence, the validity of the measured results is confirmed.

Figure 15 shows the variations of the input resistance due to temperature changes. In the simulation, an input resistance with infinite conductivity was used as the value at a temperature of absolute zero. In the conventional structure, the measured and simulated results agree well at room temperature and cooled temperature. In the folded structure, the measured results are about 5 Ω lower than the simulation results. Next, in consideration of the temperature variations of the ohmic resistance, the ohmic resistance is estimated. When the structure is cooled to –144 °C, the reduction ratio of the ohmic resistance is 0.46 times the value at room temperature [12]. The temperature variations of the input resistance are as follows:

$$R_{in}(\text{room temperature}) = R_r + R_l(\text{room temperature})$$

$$R_{in}(\text{cooled}) = R_r + R_l(\text{cooled}) \qquad (10)$$

When the measured values are substituted into Eq. (10), we obtain $R_r = 5.1\Omega$, $R_l(\text{room}) = 1.4\Omega$, and $R_l(\text{cooled}) = 0.7\Omega$ for the conventional structure. For the folded structure, we obtain $R_r = 23.8\Omega$, $R_l(\text{room}) = 1.7\Omega$, and $R_l(\text{cooled}) = 0.8\Omega$.

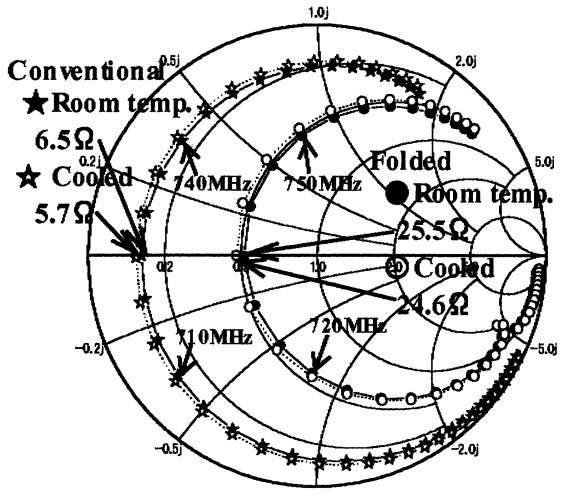

Fig. 14. 0.1 λ input impedances.

4.2. Measured radiation characteristics

Figure 16 shows the measured radiation characteristics. The antenna orientation is also plotted. The measurement plane is that containing the meander line structure. The measured polarization is oriented toward the circular periphery in Fig. 16. The directivity is of figure-8 shape like that for the dipole antenna. It is found that the antenna has an infinitesimal current source oriented in the side direction. When the conventional type and the folded type are compared, gain improvements of 3.7 dB at room temperature and 3.4 dB at cooled temperature are obtained. The peak level increases by somewhat less than 0.5 dB with cooling.

4.3. Summary of 0.1 λ antenna

Table 1 summarizes the measured and calculated results for the 0.1 λ antenna. The measured resistance value is the same as that in Fig. 14. Good correspondence is seen

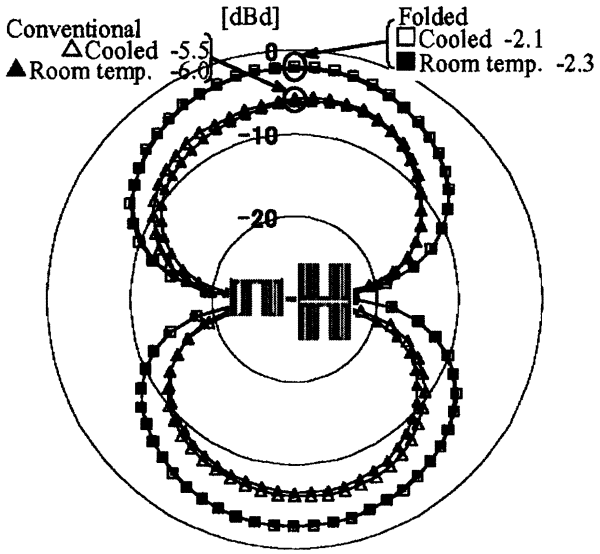

Fig. 16. Radiation pattern of 0.1 λ.

between the input resistances of the conventional type and the folded type. By using the estimated value of the ohmic resistance derived in Fig. 15, the measured and computed results can be compared. In the case of the conventional structure, the values estimated from the measurements are $R_r = 5.1\Omega$ and $R_l = 1.4\Omega$ and the computed values are $R_r = 5.6\Omega$ and $R_l = 2.5\Omega$ so that the agreement is good. In the case of the folded type, the values estimated from the measurements are $R_r = 23.8\Omega$ and $R_l = 1.7\Omega$, but the computed values are $R_r = 26.0\Omega$ and $R_l = 4.9\Omega$, so that the agreement is fair. As a result of the above discussions, the validity of simulation and measured resistances can be guessed.

Table 1. Summary of input resistances and gains

			Measurements	Simulation
			Rin (Rr+Rl) [Ω]	
Input resistances	Conventional	Room temp.	6.5	8.1 (5.6+2.5)
		Cooled	5.7	—
	Folded	Room temp.	25.5	30.9 (26.0+4.9)
		Cooled	24.6	—
			[dBd]	
Gains	Conventional	Room temp.	-5.99	-5.2
		Cooled	-5.53	—
	Folded	Room temp.	-2.28	-1.5
		Cooled	-2.08	—

With regard to the antenna gain, the measured and computed values agree well for the conventional type. In the folded type, the measured result is about 0.8 dB lower. Nevertheless, an antenna gain of –2.3 dBd is obtained, which is considered satisfactory in view of the fact that a half-wave antenna is reduced to 1/5.

5. Trial Fabrication of 0.05 λ Antenna

Figure 17 shows the configuration of a 0.05 λ antenna. The width of the conductors to be fed is set at 0.2 mm (4.7×10^{-4} λ). In order to keep the ohmic resistance as small as possible, the folded conductor width is twice as large at 0.4 mm (9.3×10^{-4} λ). The step-up ratio of the radiation resistance becomes 5.6. Each configuration with different conductor widths is designed so that they resonate at 700 MHz. Figure 18 shows a fabricated antenna. The antenna element cannot maintain a flat shape because copper film with a thickness of 35 μm (8.2×10^{-5} λ) is etched on an extremely thin plastic film. Hence, it is fixed on an OHP film, which has satisfactory strength. The center gap of the copper film is soldered to a coaxial cable with 2.5 mm ϕ.

5.1. Measured results of input resistance

Figure 19 shows the measured input impedance. Cooling efficiency is increased by dripping liquid nitrogen vapor directly onto the antenna element. The Styrofoam container for cooling is reduced in size according to the antenna size and the sealing of the container is improved. Thus, the dwell time of the nitrogen vapor becomes longer and the antenna temperature can be reduced to –196 °C, close to the temperature of liquid nitrogen. By converting the conventional configuration to the folded configuration, the input resistance is found to be increased at both room temperature and the cooled temperature. Figure 20 shows

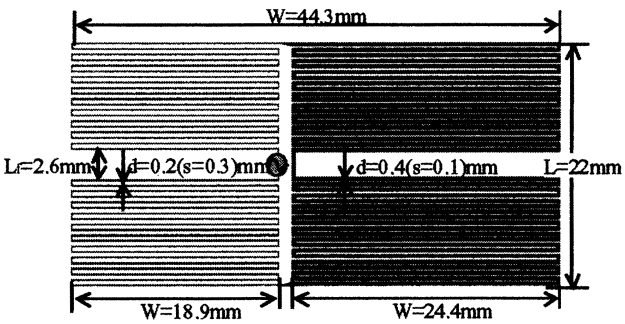

Fig. 17. Structure of 0.05 λ folded antenna ($N = 38$).

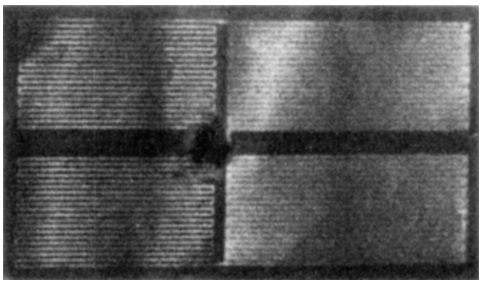

Fig. 18. Manufactured 0.05 λ folded antenna.

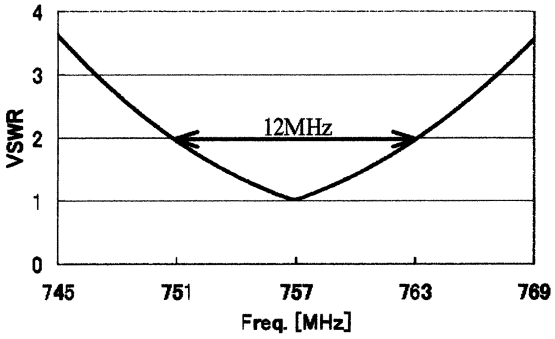

Fig. 20. VSWR of 0.05 λ.

the bandwidth of the folded type at room temperature (20 °C). The frequency bandwidth for VSWR < 2 is 12 MHz, or 1.6% in relative bandwidth. Figure 21 shows the variations of the input resistance versus environment temperature. For both the conventional and folded configurations, the measured and computed values agree well at room temperature and on cooling. Next, in consideration of the temperature change of the ohmic resistance, estimated values of the ohmic resistance are obtained. When antennas are cooled to –196 °C, the ohmic resistance is 0.17 times the value at room temperature [12]. The temperature variations of the input resistance are as follows:

$$R_{in}(\text{room temperature}) = R_r + R_l(\text{room temperature})$$

$$R_{in}(\text{cooled}) = R_r + R_l(\text{cooled}) \qquad (11)$$

When the measured results are substituted into Eq. (11), we obtain $R_r = 3.3\ \Omega$, $R_l(\text{room}) = 10.2\Omega$, and $R_l(\text{cooled}) = 1.7\Omega$ for the conventional structure and $R_r = 15.8\Omega$, $R_l(\text{room}) = 32.9\Omega$, and $R_l(\text{cooled}) = 5.6\Omega$ for the folded structure.

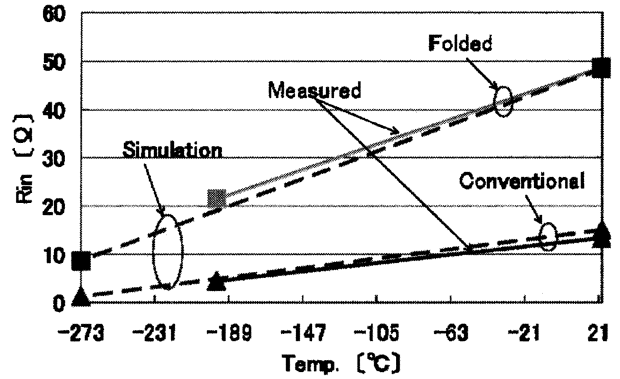

Fig. 21. Temperature versus input resistance (0.05 λ).

5.2. Measured radiation characteristics

Figure 22 shows the measured radiation characteristics. In the conventional type, the gain was –12 dBd. By using the folded type, the gain was improved by 2 dB to –10 dBd. Also, the gain is improved by cooling to –8

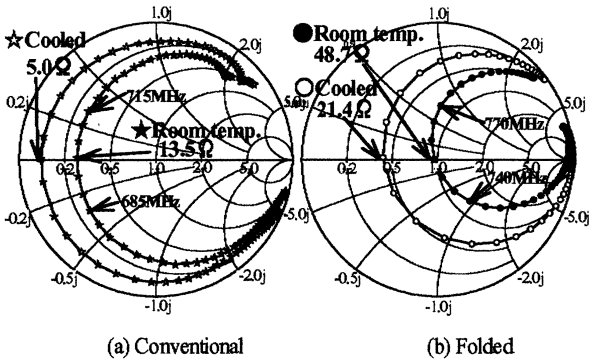

Fig. 19. Input impedance of 0.05 λ.

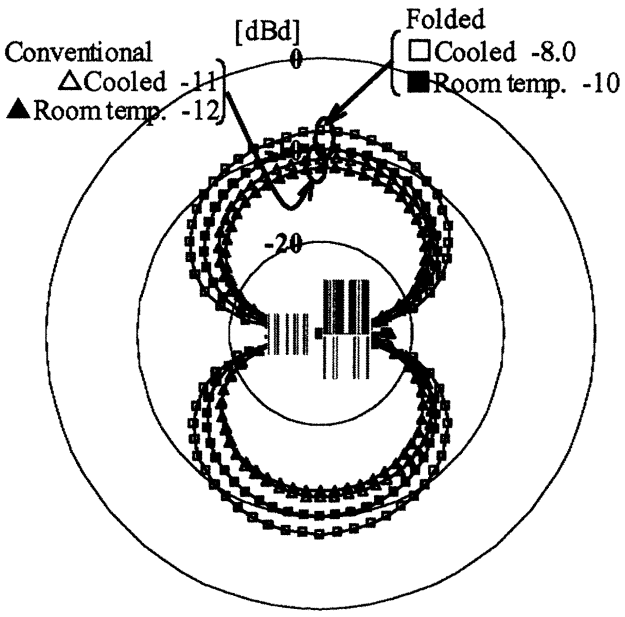

Fig. 22. Radiation pattern of 0.05 λ.

Table 2. Summary of input resistances and gains (0.05 λ)

			Measurement	Simulation
			Rin (Rr+Rl) [Ω]	
Input resistances	Conventional	Room Temp.	13.5	15.1 (1.2+13.9)
		Cooled	5.0	—
	Folded	Room Temp.	48.7	48.6 (8.6+40.0)
		Cooled	21.4	—
			[dBd]	
Gains	Conventional	Room Temp.	-12	-12.9
		Cooled	-11	—
	Folded	Room Temp.	-10	-8.0
		Cooled	-8.0	—

dBd. This suggests the existence of a substantial ohmic loss. In comparison with the 0.1 wavelength antenna, the conductor width (d) is reduced by 1/8.5, from 1.7 mm to 0.2 mm, so that the ohmic loss increases at least 8.5 times. Hence, the gain is reduced from –2 dBd to –10 dBd.

5.3. Summary of 0.05 λ antenna

The measured and computed results for the 0.05 λ antenna are summarized in Table 2. The measured resistances are reproduced from Fig. 19. With regard to the input resistances, the measured and computed results agree well for both the conventional and folded structure at room temperature. Next, the estimated values in Fig. 21 derived with allowance for the temperature change of the ohmic resistance are compared with the computed values. In the conventional structure, the estimated values are $R_r = 3.3\Omega$ and $R_l = 10.2\Omega$ and the computed values are $R_r = 1.2\Omega$ and $R_l = 13.9\Omega$. The estimated and computed values agree rather well. In the folded structure, the estimated values are $R_r = 15.8\Omega$ and $R_l = 32.9\Omega$ and the computed values are $R_r = 8.6\Omega$ and $R_l = 40\Omega$. The radiation resistance of the estimated value is twice the computed value. The magnitude of the estimated R_r is too great when the antenna gain (–10 dBd) in Table 2 is taken into account. In the method of calculating the ohmic loss with allowance for the temperature variation of the ohmic loss, the result strongly depends on the temperature coefficient of the ohmic loss (0.17). If the temperature coefficient is 0.3, then the estimated values become $R_l = 39\Omega$ and $R_r = 9.7\Omega$, which agree well with the computed values. The temperature coefficients in Ref. 12 are the values for a DC current. Further studies are needed, including confirmation at higher frequencies. With regard to the gain, the measurements and simulation results for the conventional structure agree well.

6. Conclusions

In research aimed at the realization of a very small meander line antenna, the structural dimensions of the antennas for sizes from 0.1 wavelength to 0.025 wavelength at resonance are obtained. In the folded structure that can improve efficiency, the differences in the step-up ratios of the radiation resistance and the ohmic resistance are explained theoretically. In addition, the numerical values of both resistances, which are the basis for the electrical characteristics, are derived. Further, antennas operating at 0.1 and 0.05 wavelength are fabricated. Comparison between the numerical values and the measured values confirms the validity of the simulation. The attainable performance is ascertained.

Acknowledgments. In the course of this research, the authors received assistance from K. Yamada of the Optowave Research Laboratory in the trial fabrication of antennas. They also thank T. Iwata and Prasad Sanchan, fourth-year students at the National Defense Academy, for experimental assistance.

REFERENCES

1. Ito H, Haruki H, Fujimoto K. A small-loop antenna for pocket-size ratio equipment. National Technical Report of Matsushita Communication Industrial Co. 1973;19:145–154.
2. Shinji M. Small or low profile antennas and radio communication systems. Trans IEICE 1988;J71-B:1198–1205.
3. Hiroi Y, Fujimoto K. Practical usefulness of normal mode helical antenna. IEEE AP-S International Symposium, p 238–241, 1976.
4. Nakano H, Tagami H, Yoshizawa A, Yamauchi J. Shorting ratios of modified dipole antennas. IEEE Trans Antennas Propag 1984;32:385–386.
5. Nebiya H, Uetake K. Ubiquitous wireless engineering and miniature scale RFID. Tokyo Denki University Press; 2003.
6. Endo T, Sunahara Y, Satoh S, Katagi T. Resonant frequency and radiation efficiency of meander line antenna. Trans IEICE 1997;J80-B-II:1044–1049.
7. Noguchi K, Shouji H, Mizusawa M, Yamaguchi T, Okumura Y. Impedance characteristics of small meander line antennas. Tech Rep IEICE 1997;A·P97-55:13–18.

8. Noguchi K, Mizusawa M, Yamaguchi H, Okumura Y, Betsudan S. Increasing the bandwidth of a small meander line antenna consisting of two strips. Trans IEICE 1999;J82-B:402–409.
9. Takiguchi M, Yamada Y. High impedance design of a very small meander line antenna. Tech Rep IEICE 2003;A·P2002-142:47–52.
10. Balanis CA. Antenna theory: Analysis and design, 2nd ed. John Wiley & Sons; 1997. p 458–462.
11. Takiguchi M, Yamada Y. Experimental confirmation of improvement of radiation efficiencies of a very small meander line antenna. Tech Rep IEICE 2003;A·P2002-113:69–74.
12. Otsuki Y, Koide S. New edition of physics information sources. Kyoritsu Publishing Co.; 1997. p 59.

AUTHORS (from left to right)

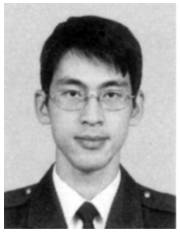

Masato Takiguchi (student member) graduated from the Department of Electronic Engineering, National Defense Academy, in 1999. After completing the Air Self Defense Officer Candidate School, he was commissioned in the 5th Air Group of the National Air Self Defense Agency. In 2002, he entered the graduate program at the National Defense Academy. Since then, he has been engaged in research on small meander line antennas. He has been affiliated with the National Air Self Defense Force since 2004.

Yoshihide Yamada (member) received his B.S. and M.S. degrees from Nagoya Institute of Technology in 1971 and 1973 and joined Nippon Telegraph and Telephone (present NTT) Research Laboratories. In 1992, he transferred to NTT Mobile Communications. In 1995, he was assigned to YRP Mobile Communication Research Laboratories. In 1998, he became a professor in the Department of Electronic Engineering, National Defense Academy. He has been engaged in research chiefly on aperture antennas, array antennas, and small antennas. In 2003, he received a Research Award from the Japan Simulation Society. He holds a D.Eng. degree (Tokyo Institute of Technology, 1989), and is a member of IEEE and the Japan Simulation Society.